Available online at www.sciencedirect.com

ScienceDirect

Procedia Materials Science 7 (2014) 79 – 86

Procedia Materials Science

www.elsevier.com/locate/procedia

2nd International Summer School on Nuclear Glass Wasteform: Structure, Properties and Long-Term Behavior, SumGLASS 2013

A Thermodynamic Approach to predict the Metallic and Oxide Phases Precipitations in Nuclear Waste Glass Melts

S. Gossé[a]*,C. Guéneau[a], S. Bordier[a], S. Schuller[b], A. Laplace[b], J.Rogez[c]

[a] *DEN,DPC,SCCME,LM2T CEA Saclay 91191 Gif-sur-Yvette, France*
[b] *DEN,DTCD,SECM,LDMC, CEA Marcoule, 30207 Bagnols-sur-Cèze, France*
[c] *IM2NP, Faculté des Sciences et Techniques – Service 262, 13397 Marseille Cedex 20, France*

Abstract

Among the large number of matrixes explored as hosts for high-level nuclear wastes, conditioning of fission products and minor actinides into a homogeneous borosilicate glass is the most promising technique already implemented at the industrial scale. The advantage of this vitrification process is the volume reduction of the high level waste coming from the spent fuel reprocessing and its stability for the long-term storage. Nevertheless, some fission products are poorly soluble in molten glasses:

- Platinoids (Pd, Ru, Rh) which precipitate as (Pd-Te, Ru-Rh) metallic particles and (Rh,Ru)O_2 oxide phases with acicular or polyhedral shapes during the vitrification process.
- Molybdenum oxide (MoO_3) which can form complex molybdates.

In order to point out the chemical interactions between the glass and these precipitated phases issuing from the calcinated waste, a thermodynamic approach is developed using the Calphad method. The objective of this work is to calculate thermodynamic properties for complex fission product systems in order to predict the precipitation of platinoids or molybdate phases.
This thermodynamic database is being developed on the Mo-Pd-Rh-Ru-Se-Te-O complex system. This flexible tool enables to predict phase diagrams, composition and relative stability of the metallic or oxide precipitated phases as a function of both temperature and oxygen potential in the glass melt.

Selection and peer-review under responsibility of the scientific committee of SumGLASS 2013

Keywords: Thermodynamic; Calphad; Nuclear Waste Glasses; Platinoid; Molybdenum; Fission product

* Corresponding author. Tel.: +33 (1) 69 08 97 39; fax: +33(1) 69 08 92 21.
E-mail address: stephane.gosse@cea.fr

Selection and peer-review under responsibility of the scientific committee of SumGLASS 2013
doi:10.1016/j.mspro.2014.10.011

1. Introduction

During vitrification process of high level radioactive glasses, slightly soluble Pd-Rh-Ru platinoid metals and molybdenum as complex oxides exhibit low loading rate (Figure 1) [1-3]. Platinoids mainly form (Pd-Te, Ru-Rh) metallic particles [1-5] and/or $(Rh,Ru)O_2$ oxide phases [3-5] in the vitreous matrix of high level waste containment glasses. At high concentration, molybdenum oxide tends to demix as a complex molybdate phase enriched mainly in sodium molybdates, calcium and other alkalines (Cs, Li) and alkaline-earth (Ca, Sr, Ba, Mg) [6-9].

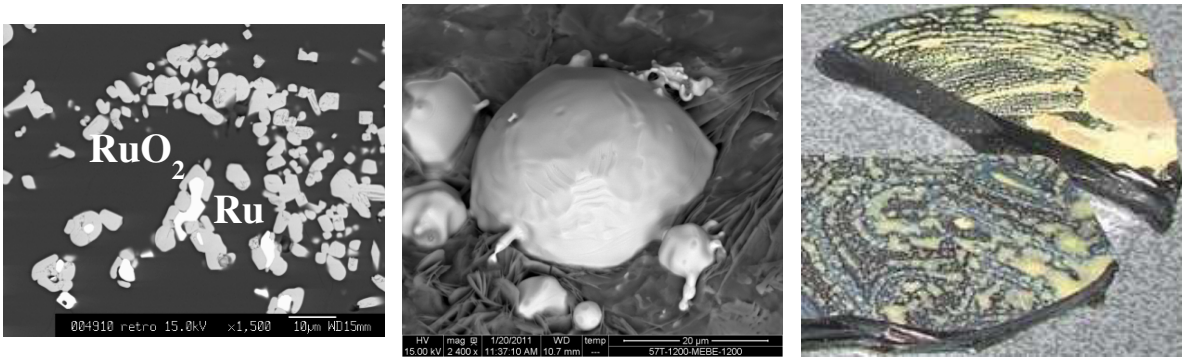

Figure 1: Crystallized metallic and oxide phases in nuclear borosilicate glasses: a) Ru-HCP and RuO_2 polyhedra, b) Pd_xTe_y Intermetallics observed by ESEM and c) Visual observation of a complex yellow phase obtained by high temperature reaction between glass frit and calcine

This paper presents the development of a thermodynamic modelling for typical nuclear waste compositions. Using the Calphad method [10], a database was developed on the Mo-Pd-Rh-Ru-Se-Te-O system. The objective is to use a thermodynamic approach to develop solution models for fission products and oxide melts systems that are predictive with regard to composition, phase separation, and volatility observed during vitrification of nuclear waste glasses.

In this work, the Gibbs free energy function of each phase (solid, liquid and gas) is modelled to provide an overall thermodynamic description of the stability of the molybdates and the platinoid phases in nuclear waste glasses:

- Because platinoids are sparingly soluble, their thermodynamic properties can be calculated without considering the glass chemistry. In this case, the melt is only taken into account through its oxygen potential.
- Concerning molybdenum, the interactions with the oxides from the melt (CaO, Na_2O, SiO_2) are considered through the assessments of the CaO-MoO_3, MoO_3-Na_2O and MoO_3-SiO_2 binary and MoO_3-Na_2O-SiO_2 ternary phase diagrams.

The main objective of the database is to calculate phase diagrams and thermodynamic properties: stability and composition of the phases at equilibrium, eutectics and demixing phenomena. This flexible tool also enables to predict the relative stability between metallic and oxide phases as a function of temperature and oxygen potential (RedOx equilibrium) somehow fixed by the glass frit.

The present thermodynamic database was used to predict the platinoid fission products and the molybdenum oxide behaviours at high temperature. These calculations partly explain the precipitation phenomena of platinoid metallic droplets and the demixing of molybdates in nuclear waste glasses.

2. Thermodynamic Modelling

To take into account the influence of platinoid and molybdate phases formed during vitrification of nuclear waste glasses, the thermodynamic approach is investigated using the Calphad method. The modelling consists in describing a complex chemical system by coupling both phase diagrams and thermodynamic properties [10,11,12].

For each (solid, liquid and gas) phase, a Gibbs energy function is defined by a polynomial function of temperature and composition. During the modelling procedure, these Gibbs energy functions are adjusted by a least-square method on the basis of experimental thermodynamic (enthalpies, activities, heat capacities, vapour pressures) or phase diagram data.

Then, for given temperature, pressure and number of component moles, the thermodynamic equilibrium is calculated by minimization of the total Gibbs free energy of the system. In the current approach, the glass phase is considered as a CaO-MoO_3-Na_2O-SiO_2 liquid solution (the glass transition is not explicitly considered). Then, phase diagrams and thermodynamic properties can be calculated by extrapolating the liquid to low temperatures.

2.1. Description of the noble metal metallic systems

In the thermodynamic description of the quaternary Pd-Rh-Ru-Te-Se system, the most relevant binary systems were modelled using critically assessed thermodynamic data from the literature. Many of these binary phase diagrams were already presented elsewhere; the Pd-Te, Pd-Ru, Rh-Ru and Rh-Te systems were investigated and modelled in the framework of previous studies [13-15], the Pd-Rh [16] and Se-Te [17] assessments come from the literature; the metal-oxygen or chalcogen-oxygen binary systems are considered too. All these descriptions were combined to calculate the thermodynamic properties of higher order systems by extrapolation of the binaries.

In the Pd-Rh-Te system, an optimization process was performed to fit the data of Hartmann et al. [21] who performed thermal treatments in this ternary system. The thermodynamic modelling considered the results obtained on annealed samples in the 1023 K-1523 K temperature range. The isothermal sections calculated at 1173 K and 1273 K are consistent with the phase equilibria experimentally observed (Figure 2a & 2b).

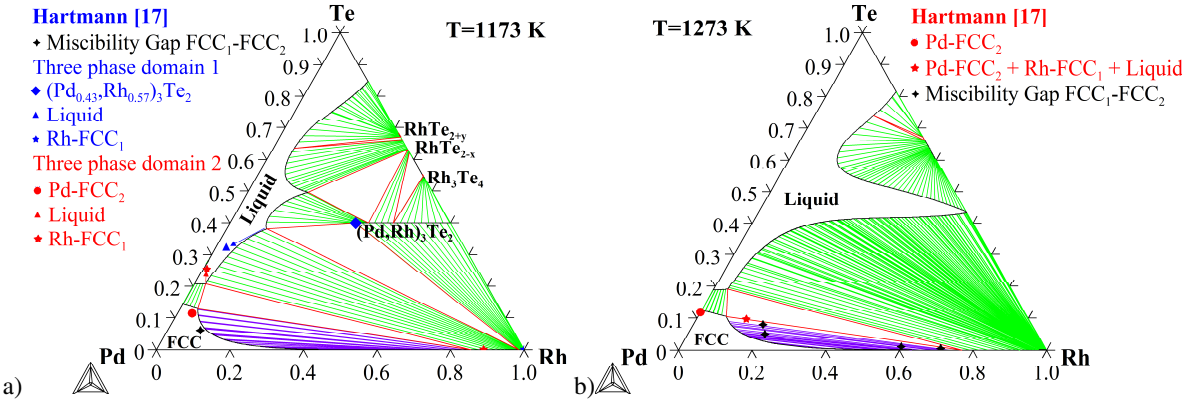

Figure 2: Pd-Rh-Te isotherms calculated at a) 1173 K and b) 1273 K. Comparison with experimental data from Hartmann et al. [21]

In the case of the Pd-Rh-Ru [18,19] system, an additional step was performed to assess this phase diagram according to Raevskaya et al. [18] and Paschoal et al. [19]. Raevskaya et al. studied the interactions of platinum group metals to establish phase relations at 1673 K [18]; the arc melted samples were annealed for 500 hours. Paschoal et al. [19] studied the Pd-Rh-Ru system at 1973 K by metallography, X-ray diffraction, and electron-probe microanalyses. Both isothermal sections calculated at 1673 K and 1973 K are consistent with these experimental results [13].

Due to the selenium tendency to form intermetallic compounds, the Pd-Se phase diagram was assessed [20] (Figure 3a). The Te-Se binary system (Figure 3b) is calculated using the assessment of Ghosh et al. [17]. The modelling of the interactions between Te, Se and Pd makes it possible to calculate Pd-Se-Te isothermal sections (Figure 4a) and to predict the thermodynamic properties of the ternary mixtures. These calculations are useful to predict the Se *vs.* Te affinity towards Pd when liquid metallic droplets form and precipitate as complex intermetallic compounds.

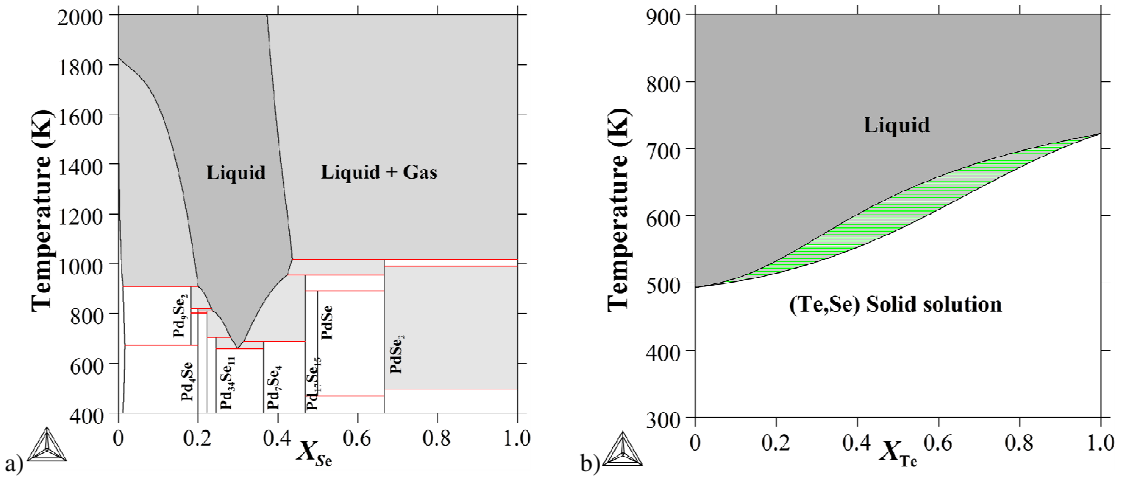

Figure 3: Calculated Pd-Se (this study) and Se-Te [17] phase diagrams. Dark grey corresponds to the single phase liquid and light grey corresponds to the two-phased liquid domains

Considering a Te/Se molar ratio of 10 typical of some nuclear waste, it is possible to calculate the respective Te and Se chemical activities (referred to the gas phase) at the glass melt temperature (1373 K) as a function of the Pd atomic fraction. As shown below (Figure 4b), Se and Te activities are negligible when the Pd-FCC solid solution is stable (see labels 2 & 3). Then, once the liquidus line crossed (see labels 1 & 4), both Te and Se activities increase but in different proportions along the Te/Se = 10 line.

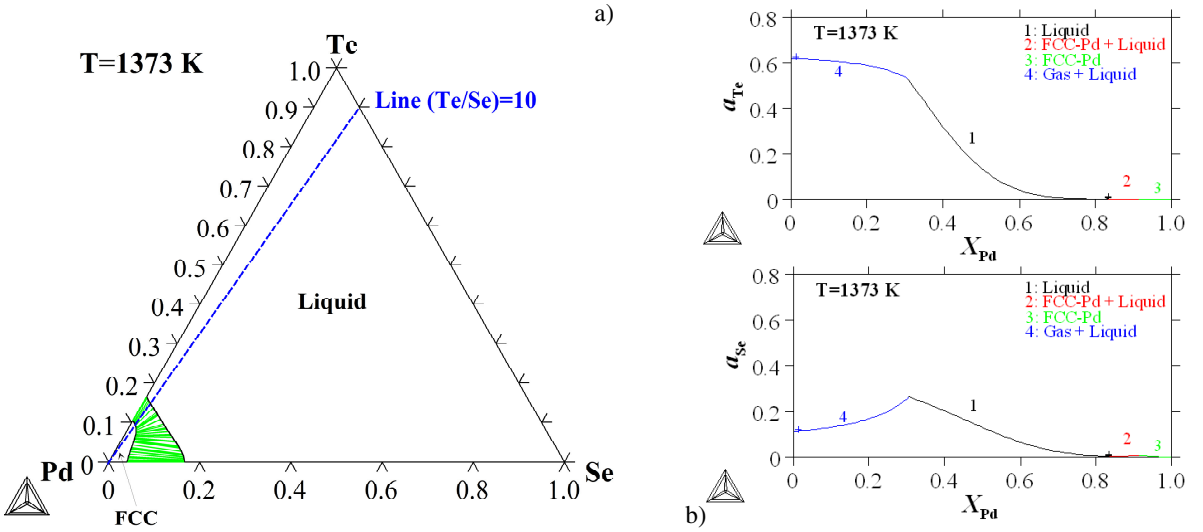

Figure 4: a) Pd-Se-Te isotherm calculated at 1373 K. b) Calculated Te and Se activities along the Te/Se=10 line (Reference states for Se and Te are gas at 1373 K)

2.2. Description of the CaO-MoO_3 and Na_2O-MoO_3 oxide systems

In order to calculate the thermodynamic properties of $CaMoO_4$ and Na_2MoO_4, the CaO-MoO_3 and Na_2O-MoO_3 systems were modelled using data from the literature. The CaO-MoO_3 phase diagram (Figure 5a) was assessed using the experimental results from Yanushkevich et al. [22]. Many other thermodynamic data were used to calculate the Gibbs energy functions of $CaMoO_4$ [23-25]. The Na_2O-MoO_3 phase diagram (Figure 5b) was assessed using phase diagram data from Caillet [26], Groshuff [27], Hoermann [28], Baloshov et al. [29] and Mudher et al. [30].

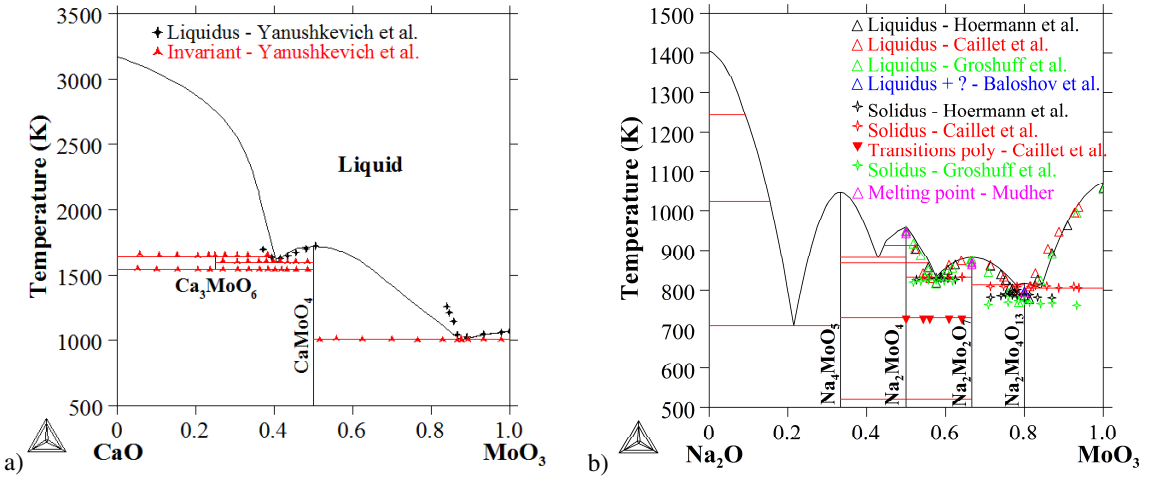

Figure 5: Calculated phase diagrams a) CaO-MoO_3 and b) Na_2O-MoO_3. Comparison with data from the literature

3. Thermodynamic Calculations

The thermodynamic database was used to predict the platinoid fission products and the molybdenum oxide behaviours at high temperature. These calculations partly explain the precipitation of platinoid metallic droplets and the molybdate formation observed in nuclear waste glasses.

3.1. Effect of RedOx on the Platinoids at equilibrium

Considering a Pd-Rh-Ru-Te-Se-O mixture, the stable phases were calculated as a function of oxygen potential (Figure 6). The retained composition corresponds to a typical waste coming from an UOX spent fuel [31]. To perform this calculation, the masses of the fission products were: SeO_2 = 77 g, RuO_2 = 2846 g, Rh = 488 g, Pd = 1245 g and TeO_2 = 592 g (usually referred to one ton of uranium). The temperature was fixed to 1473 K in order to be representative of the glass melt.

Then, the RedOx effect was studied by subtracting or adding some fictitious oxygen to this chemical system at 1473 K. At low oxygen potential $-5 < \log_{10} p(O_2) < -1.8$ (p in bar), the main phases at equilibrium are the HCP-Ru solid solution and a metallic liquid in which all the other elements are solubilised. Then, the increase of oxygen pressure ($-1.8 < \log_{10} p(O_2) < -1.4$) reveals the formation of RuO_2 due to the oxidation of HCP-Ru. The metallic liquid is still stable and gas appears. At 1473 K, the precise calculated Ru/RuO_2 RedOx ($\log_{10} p(O_2)$) is equal to -1.934. Finally, at high oxygen potential $-1.4 < \log_{10} p(O_2) < 0$, the main phases at equilibrium are RuO_2, the metallic liquid and the FCC-(Pd,Rh) solid Solution.

At 1473 K, the oxygen pressure in the glass melt is about $\log_{10} p(O_2) \approx -0.4$. Under these conditions, the predicted platinoid phases correspond to the experimental observations: RuO_2, the FCC-(Pd,Rh) solid solution and the metallic liquid. At this oxygen pressure, the proportion of gas begins to be important. This contribution is synonymous with vaporisation phenomena due to the formation of Se, Te and Ru oxide gaseous species: $SeO_{2(g)}$, $TeO_{2(g)}$, $Te_2O_{2(g)}$, $TeO_{(g)}$, $SeO_{(g)}$ and $RuO_{3(g)}$. These calculations are in good accordance with the experimental results from the studies performed on platinoid insoluble fines in nuclear waste glasses [32-34].

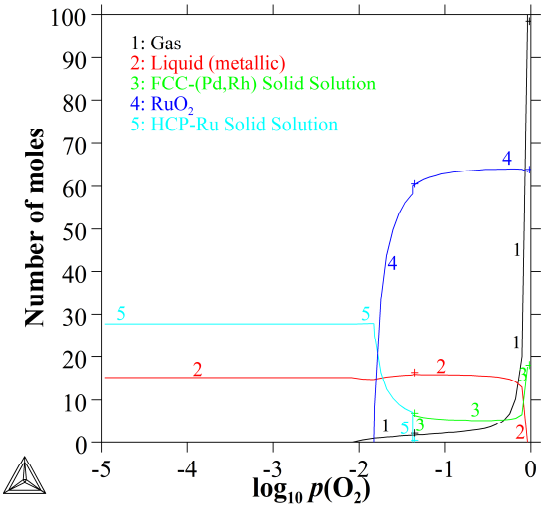

Figure 6: Calculated stable phases at equilibrium as a function of $\log_{10} p(O_2)$ in bar. Temperature is fixed to 1473 K

3.2. Demixing of calcium molybdates in the Na_2O-MoO_3-SiO_2 ternary system

The phase separation of calcium and sodium molybdates in simplified complex glass waste forms were studied thoroughly [34-37]. Nevertheless, the thermodynamic approach was rarely retained to explain this phenomenon. In their studies, Stemprok et al. [37-39] determined the liquid miscibility gap. This demixing phenomenon is partly responsible for the precipitation of Na_2MoO_4 in this simple silicate melt.

On the thermodynamic point of view, the demixing phenomena in complex liquids can be explained and modelled using the Calphad method. These phase separations may occur between two insoluble metallic, oxide or metallic/oxide liquids. To build the Na_2O-MoO_3-SiO_2 ternary system, the present assessment of the Na_2O-MoO_3 system (Figure 5b) and the Na_2O-SiO_2 assessment by Zhang et al. [40] (Figure 7a) were used. No experimental data was found on the MoO_3-SiO_2 phase diagram.

At high temperature (1473 K), both Na_2O-MoO_3 and Na_2O-SiO_2 systems exhibit a single liquid phase. Consequently, the demixing behavior of molybdates necessarily comes from the MoO_3-SiO_2 system. This binary liquid was modelled to reproduce a miscibility gap using a repulsive interaction parameter between the MoO_3 and the SiO_2 liquid species (+70 kJ/mol/at). The obtained phase diagram is illustrated in Figure 7b.

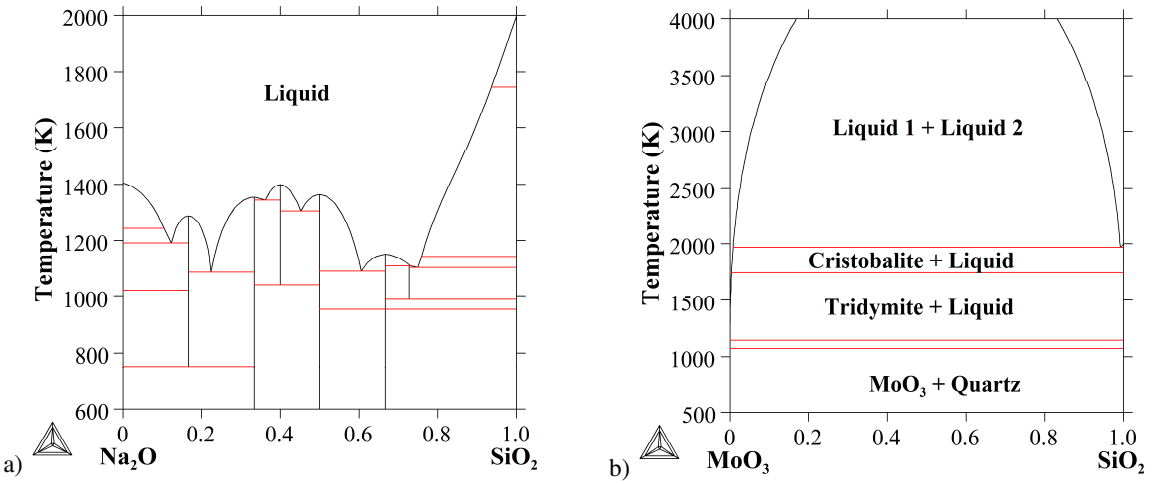

Figure 7: a) Na_2O-SiO_2 phase diagram by Zhang et al. [40]. b) Calculated the MoO_3-SiO_2 phase diagram with repulsive interactions

between MoO_3 and SiO_2 liquid species

Then the Na_2O-MoO_3-SiO_2 ternary system was optimized on the only data found in the literature; miscibility gap measurements by Stemprok et al. [37-39] at 1473 K and 1673 K. The calculated isothermal sections show that the extent of the miscibility gap varies slightly with temperature. At low temperature the two-liquid domain separates in a phase enriched in SiO_2 and Na_2O and depleted in MoO_3. This phase corresponds to the major metastable vitreous phase .The second phase enriched in MoO_3 and Na_2O and depleted in SiO_2 then crystallizes to form Na_2MoO_4.

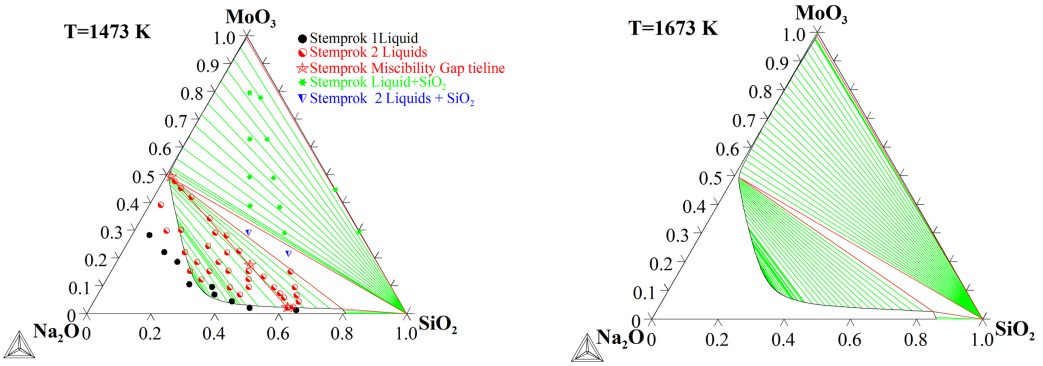

a) b)

Figure 8: MoO_3-Na_2O-SiO_2 isothermal sections calculated at a) 1473 K and b) 1673 K. Comparison with data from Stemprok et al. [37-39]

4. Conclusion

Using the Calphad method, a thermodynamic database is being developed on *i*) metallic or oxide phases issuing from fines solution and on *ii*) Ca and Na molybdates. This database takes into account platinoids Pd-Rh-Ru and Te-Se fission products, CaO-MoO_3 and Na_2O-MoO_3 molybdate systems are considered too. To take into account the effect of the oxygen pressure on the behaviour of the formed phases, the interactions between oxygen and the Pd-Rh-Ru-Te-Se elements are calculated. In the case of molybdenum, a miscibility gap arising from the MoO_3-SiO_2 liquid phase makes it possible to calculate the demixing phenomena and the precipitation of molybdates.

Using this database, some application calculations performed on platinoid phases and molybdate systems are consistent with the phenomena observed during glass formulation or vitrification studies. These results show that the thermodynamic approach can be considered as an efficient tool to better understand the precipitation of insoluble phases in nuclear glass waste forms.

Acknowledgements

This work was financed by the commissariat à L'Energie Atomique et aux Energies Alternatives. Financial support by AREVA is also gratefully acknowledged. The authors thank J. Ravaux for performing ESEM analyses at the ICSM (Marcoule, France).

REFERENCES

1. H. Mitamura, T. Murakami, T. Banba, Y. Kiriyama, H. Kamizono, M. Kumata, S. Tashiro, Nuclear and Chemical Waste Management 4 (1983)
2. A. V. Belyaev, Journal of Structural Chemistry 44, 1 (2003)
3. L. Galoisy, G. Calas, G. Morin, S. Pugnet, C. Fillet, J. Mater. Research 13, 5 (1998)
4. Ch. Krause, B. Luckscheiter, Journal of Materials Research 6, 12 (1991)
5. R. Pflieger, L. Lefebvre, M. Malki, M. Allix, A. Grandjean, J. Nuclear Mater. 389, 3 (2009)
6. R.J. Short, R.J. Hand, N.C. Hyatt, Mat. Res. Soc. Symp. Proc., (757) 141-146 (2003)

7. R.J. Short, R.J. Hand, N.C. Hyatt, Mat. Res. Soc. Symp. Proc., (807), 169-74 (2004)
8. R.J. Short, R.J. Hand, N.C. Hyatt, G. Möbus, Journal of Nuclear Material 340, 179-186 (2005)
9. L. Pegg, H. Gan, K. S. Matlack, Y. Endo, T. Fukui, A. Ohashi, J. Innocent, B. W. Bowan, WM-2010 Conference, March 7-11, Phoenix, USA (2010)
10. H. Lukas, S. G. Fries, B. Sundman, Cambridge University Press, Cambridge UK (2007)
11. B. Jansson, Ph D thesis, Royal Inst. Techn., Stockholm, Sweden: KTM (1984)
12. B. Sundman, B. Jansson, J-O.Andersson, Calphad 9 (1985)
13. S. Gossé, S. Schuller, C. Guéneau and H. Boucetta, MRS Proceedings 1369 (2011)
14. S. Gossé, C. Guéneau, Intermetallics 19, 5 (2011)
15. S. Gossé, S. Schuller, C. Guéneau, MRS Symposium Proceedings 1265 (2010)
16. R. Gürler, Journal of Nuclear Materials 199 (1992)
17. G. Ghosh, R. C. Sharma, D. T. Li, Y. A. Chang, Journal of Phase Equilibria 15 (1994)
18 M. V. Raevskaya, V. V. Vasekin, I. G. Sokolova, J. of the Less Com. Met. 99 (1984)
19. J. O. A. Paschoal, H. Kleykamp, F. Thümmler, Zeitschrift Für Metallkunde 74, 10 (1983)
20. S. Bordier, A. Chocard, S. Gossé, Journal of Nuclear Materials 451, pp. 120–129 (2014)
21. T. Hartmann, H. Pentinghaus, Journal of Nuclear Materials 422, pp. 124–130 (2012)
22. T. Yanushkevich, V. Zhukovskii, Zhurnal Neorganicheskoi Khimii 18 (1973)
23. W. W. Weller, E. G. King, Bureau of mines, Report of investigations (1963)
24. A. P. Zhidikova, O. L. Kuskov, Trans. from Geokhimiya, pp. 1149-1151 (1971)
25. R. Saha, R. Babu, K. Nagarajan, C. Mathews, Journal of Nuclear Materials 167 (1989)
26. P. Caillet, Bulletin de la Société Chimique de France. 12 (1967)
27. E. Groschuff, Z. Anorg. Allg. Chem. 58, 113 (1908)
28. F. Hoermann, Z. Anorg. Allg. Chem. 177, 145 (1929)
29. V. A. Baloshov, A. A. Maier, Neorganicheskie Materialy 6, 1450 (1989)
30. K. S. Mudher, M. Keskar, K. Krishnan, V. Venugopal, J. Alloys Comp. 396, 275 (2005)
31. N. Chouard, Ph. D Thesis, Université Pierre et Marie Curie, Paris (2011)
32. O. Pinet, S. Mure, Journal of Non-Crystalline Solids 355, pp. 221-227 (2009)
33. O. Pinet, R. Boën, Journal of Nuclear Materials (2014), DOI: http://dx.doi.org/10.1016/j.jnucmat.2014.01.008
34. P. B. Rose, D. I. Woodward, M. I. Ojovan, N. C. Hyatt, W. E. Lee, Journal of Non-Crystalline Solids 357 (2011)
35. M. Magnin, S. Schuller, C. Mercier, J. Trebosc, D. Caurant, O. Majerus, F. Angeli, T. Charpentier, J. Am. Ceram. Soc., 94 pp. 4274-4282 (2011)
36. S. Schuller, O. Pinet, A. Grandjean, T. Blisson, Journal of Non-Crystalline Solids 354 pp. 296–300 (2008)
37. S. Schuller, O. Pinet, B. Penelon, Journal of the American Ceramic Society, 94 (2) pp. 447-454 (2011)
38. M. Stemprok, J. Voldan, Silikaty 18, pp. 19-30 (1974)
39. M. Stemprok, International Geology Review 17, pp. 1306-1316 (1975)
40. L. Zhang, C. Schmetterer, P. J. Masset, Computational Materials Science 66 pp. 20–27 (2013)